Microscopic look at the nuclear twist

B. Schwesinger
Institut für Kernphysik, Kernforschungsanlage Jülich, D-5170 Jülich, Federal Republic of Germany and Department of Physics, State University of New York at Stony Brook, Stony Brook, New York 11794
(Received 3 October 1983)

For ^{90}Zr and ^{208}Pb a microscopic one-particle-one-hole plus two-particle-two-hole calculation examines fluid dynamical predictions about a collective twist resonance in finite nuclei at $E \sim 45A^{-1/3}$ MeV. A spin flip mode which strongly competes with the twist in experiments is heavily fragmented, thus allowing experimental detection of the twist.

I. INTRODUCTION

One of the more exotic nuclear resonances that has been speculated upon[1] is the nuclear twist. Its motion can be visualized as a rotation of the different layers of a Fermi fluid against each other, the angle of rotation (around the z axis) being proportional to the z coordinate of the layer.

Such a motion is expressed most easily through an operator of the form

$$\hat{T}_{T=0}=\sqrt{3/2}\sum_{i=1}^{A} z_i l_{z_i}=\sum_{i=1}^{A}[\vec{r}_i\times\vec{1}_i]_{2,m=0} \tag{1}$$

acting on the corresponding ground state. For spherical nuclei $\hat{T}_{T=0}$ excites states with the quantum numbers $J^\pi,T=2^-,0$ which in principle are detectable by inelastic electron scattering as $M2$ resonances.[2] Since the electromagnetic spin flip operator

$$\hat{S}_{\rm em}=\sqrt{15/2\pi}\mu_{\rm N}\sum_i\left[\frac{g_{\rm p}+g_{\rm n}}{2}+\tau_i^0\frac{g_{\rm p}-g_{\rm n}}{2}\right]\times[\vec{r}_i\times\vec{\sigma}_i]_{2,m=0} \tag{2}$$

contributes about 80% to the electromagnetic $M2$ sum and since twist as well as spin flip states are expected to be located around the same excitation energy, the twist mode is believed to stand in the shadow of the spin flip excitations. One purpose of this paper is to reexamine these findings[2] with a microscopic particle-hole calculation, which will allow more definite statements on the position of individual levels as compared to the sum rule approach in Ref. 2.

In a fluid dynamical description the velocity field of the twist mode is purely rotational. Such a motion is only possible if there are tangential restoring forces effective in the fluid. In order to allow for tangential forces the pressure tensor

$$\Pi_{ik}(\vec{r},t)=m\int p_i p_k n(\vec{r},\vec{p},t)d^3p \tag{3}$$

in the fluid must be nonisotropic. This implies that the partition function $n(\vec{r},\vec{p},t)$ contains a second rank tensor part in the momentum variable p.

In a fluid where particles suffer frequent collisions among each other the pressure tensor will be diagonal and isotropic because frequent collisions will enforce a spherical momentum distribution. Therefore the existence of the nuclear twist will indicate the propagation of a collisionless mode, which can be viewed as transverse zero sound.

Since frequent collisions are a mechanism to attenuate a transverse zero sound wave, the particle-hole calculation we present includes the effects of 2p-2h states (in the same way as in Ref. 3). This should enable a realistic prediction of whether a microscopic theory allows for the propagation of spinless transverse excitations in a finite Fermi system.

The paper is organized as follows. In Sec. II we derive some features of zero sound modes from solutions of (a truncated) version of the Landau theory.[4] We present the solutions for a spherical basis which to our knowledge is new. These allow us to understand many features of the numerical microscopic calculation outlined in Sec. III. Section IV presents and discusses the numerical results for the nuclei ^{90}Zr and ^{208}Pb. A comparison to the data on $M2$ strength distributions from the Darmstadt LINAC group[5,6] is also included.

II. FLUID DYNAMICAL APPROACH

The Landau theory assumes that changes in the partition function $n(\vec{r},\vec{p},t)$ are driven by quasiparticle energies $\epsilon_{\vec{p}}$ and a collision term (see, e.g., Ref. 7). We are interested in small deviations δn from the ground state solution n_0. These changes occur for momenta near the Fermi momentum. We set

$$\delta n=\frac{\partial n_0}{\partial\epsilon_p}\nu(\vec{r},\vec{p},t)\ , \tag{4}$$

such that the restriction of the momenta in δn to the Fermi momentum is expressed by the derivative $\partial n_0/\partial\epsilon_p$ [which actually is $\sim\delta(\epsilon_p-\epsilon_F)$].

Neglecting the collision integral and all surface terms, which we will later replace by a suitable boundary condition, the equation of motion for ν is given by[7]

$$\frac{\partial}{\partial t}\nu(\vec{p},\vec{r},t)+\frac{1}{m^*}\vec{p}\cdot\nabla\bar{\nu}(\vec{p},\vec{r},t)=0\ . \tag{5}$$

m^* is the effective mass at the Fermi surface

$$\nabla_p\epsilon_p=\frac{1}{m^*}\vec{p}\ \text{for}\ p=p_F\ . \tag{6}$$

$\bar{\nu}$ abbreviates the change of the partition function plus the changes induced by the particle hole interaction (parametrized by the F_K),

$$\bar{\nu}(\vec{p},\vec{r},t)=\nu(\vec{p},\vec{r},t)+\sum_{KM}\frac{F_K}{2K+1}Y_{KM}(\hat{p})\times\int Y^*_{KM}(\hat{p}')\nu(\vec{p}\,',\vec{r},t)d\hat{p}'\ . \tag{7}$$

Solutions of (5) are readily obtained for the infinite matter case as plane waves.[4,7]

For our purposes the solutions of (5) in a spherical basis are more useful and may be obtained by either direct calculation or by projection of the plane wave solutions of definite rotational transformation properties. Both procedures yield

$$\nu^{J^\pi,m}_{\omega,q}(\vec{r},\vec{p},t)=\sum_{K,L}\frac{1+\pi(-)^{K+L}}{2}[e^{-i\omega t}+(-)^{K+J}e^{i\omega t}]a^m_K(s)\sqrt{(2K+1)(2L+1)}\begin{bmatrix}K & L & J\\ -m & 0 & m\end{bmatrix}i^L j_L(qr)\times[Y_K(\hat{p})\times Y_L(\hat{r})]_{J,M=0}\ , \tag{8}$$

where J specifies the multipolarity, π the parity, and q the wave number of the excitation. $j_L(x)$ is a spherical Bessel function and the tensorial product $\times$ in (8) denotes coupling to a spherical tensor of rank J,M with the appropriate Clebsch-Gordan coefficients. $M=0$ has been chosen for the sake of a simple expression for real ν. The frequency ω is related to the wave vector q and the sound velocity s via

$$\omega=\frac{1}{m^*}p_F s q\ . \tag{9}$$

The amplitudes $a^m_K(s)$ are the eigenvectors of the infinite eigenvalue problem

$$\sqrt{(K-m)(K+m)}\left[1+\frac{F_{K-1}}{2K-1}\right]a^m_{K-1}(s)-(2K+1)sa^m_K(s)+\sqrt{(K-m+1)(K+m+1)}\left[1+\frac{F_{K+1}}{2K+3}\right]a^m_{k+1}(s)=0 \tag{10}$$

given in Ref. 4 and s is its eigenvalue. These amplitudes and the sound velocity do not depend on the parity and the multipolarity of the excitation.

The index m labeling the solutions in (8) and (9) distinguishes different kinds of modes, where the two lowest $m=0,1$ will be of interest to us. Consider the transition density of an excitation

$$\rho^{J^\pi,m}(\vec{r})\sim\int\nu^{J^\pi,m}_{\omega,q}(\vec{r},\vec{p},t)d\hat{p}\ , \tag{11}$$

which apart from a factor is just given by the $K=0$ term of the sum (8). Because of the 3-j symbol only $m=0$ contributes to the zeroth moment $K=0$, so $m=0$ is the only mode of the system involving a change in density; this must be identified with a longitudinal excitation.

Similarly by looking at the transition currents

$$\vec{j}^{\,J^\pi,m}(\vec{r})\sim\int\hat{p}\nu^{J^\pi,m}_{\omega,q}d\hat{p}\sim a^m_1(s)\sum_L\frac{1+\pi(-)^{L+1}}{2}\sqrt{2L+1}\begin{bmatrix}1 & L & J\\ -m & 0 & m\end{bmatrix}i^L j_L(qr)\vec{Y}_{JL0}(\hat{r})\ , \tag{12}$$

we see that only $m=0$ and $m=1$ give nonvanishing contributions (the $\vec{Y}_{JL0}$ are vector spherical harmonics as defined, e.g., in Ref. 8). The $m=0$ current is irrotational and its divergence yields the transition density. This can be seen by taking the zeroth moment of Eq. (5) which yields a continuity equation. The $m=1$ current is divergenceless and shows a nonvanishing curl. Therefore the $m=1$ modes correspond to transverse excitations of the fluid. The transition currents (12) are related to the pressure tensor defined in (3) by the Euler equation. This follows by taking the first moment in $\hat{p}$ of Eq. (5). Higher modes $m>1$ have no change in density nor any flow of matter, and are beyond the scope of this work.

It is worthwhile mentioning that the transverse $m=1$ modes allow for unnatural parity excitations: for $m=1$, the condition $(-)^{K+L+J}=1$ is no longer enforced by the 3-j symbol in (8) which then allows $(-)^J\neq\pi$. Therefore the Landau theory also describes propagation of unnatural parity modes, an example of which is the twist. With $J^\pi=2^-$ its transition density vanishes and the currents follow via (12) as

$$\vec{j}^{\,2^-}(\vec{r})\sim j_2(qr)\vec{Y}_{220}\sim\vec{r}\times\nabla z^2\frac{j_z(qr)}{(qr)^2}\ . \tag{13}$$

The connection to the operator defined in (1) is made by displacing the ground state wave functions by an amount $\vec{s}(\vec{r})$ with $\vec{s}=-\vec{j}$.

Let us now turn to the zero sound velocities which occur as eigenvalues of Eq. (10). For zero sound or transverse zero sound to propagate, the eigenvalues s^m must be real, a condition depending on the actual numbers for the Landau parameters F_K. Such information is hardly available from nuclear excitations. It has, however, been shown rather convincingly in a series of papers by Holzwarth and collaborators[1,4,9] that a "fluid dynamical" truncation scheme gives an excellent account of many nuclear excitation phenomena. This truncation scheme implies that all higher moments $a_K^m(s)$ vanish for $K>2$ (the "hydrodynamical" first sound follows from vanishing moments for $K>1$). The resulting velocities are

$$s^0=[\tfrac{1}{15}(9+5F_0+\tfrac{4}{5}F_2)(1+\tfrac{1}{3}F_1)]^{1/2} \text{ for } m=0\,,$$
$$s^1=[\tfrac{1}{5}(1+\tfrac{1}{3}F_1)(1+\tfrac{1}{5}F_2)]^{1/2} \text{ for } m=1\,, \tag{14}$$

where the transverse sound velocity s^1 is independent of F_0. F_0 is related to the compressibility of the fluid, F_1 is related to the effective mass of the quasiparticles, and F_2 seems to be negligible for nuclear excitations.[4]

Apart from the truncation, which might find its justification in the fact that we are dealing with a finite system, everything said so far applies to the infinite case as well, since we have neglected the surface terms. We replace these by requiring a boundary condition: All forces acting on the surface of a sphere of radius R must vanish. Here we assume that all particles are confined to the inside of the sphere. This means that the pressure tensor in the direction of any radially oriented surface element must vanish at $r=R$,

$$\Pi\cdot\hat{R}=\int(\vec{p}\cdot\hat{R})\vec{p}\bar{n}(\vec{r},\vec{p},t)d^3p_{r=R}=0\,. \tag{15}$$

Such a condition cannot be fulfilled for arbitrary wave vectors q and thus it determines the eigenfrequencies of the system. Furthermore, (15) will mix longitudinal and transverse modes if both can coexist in a particular excitation. Obviously (15) involves the moments $K=0$ and $K=2$ only.

For the case of the twist modes Eq. (15) [using (8) and (9)] determines the eigenvalue ω via

$$j_1\left[\frac{m^*\omega R}{p_F s^1}\right]-3j_3\left[\frac{m^*\omega R}{p_F s^1}\right]=0\,. \tag{16}$$

With (14) and $F_2=0$,

$$\omega_{\text{twist}}=2.3\frac{p_F s^1}{m^* R}=2.3\frac{p_F}{m^*}[\tfrac{1}{5}(1+\tfrac{1}{3}F_1)]^{1/2}\frac{1}{r_0}A^{-1/3}$$
$$\sim 45A^{-1/3}\text{ MeV}\,, \tag{17}$$

which is independent of F_0. Other modes such as natural parity monopole and quadrupole excitations may be obtained in a similar way and coincide with the fluid dynamical results of Ref. 9.

III. MICROSCOPIC APPROACH

In contrast to the fluid dynamical approach of the preceding section the microscopic formalism is less involved since we are just asking about the response of a nucleus to the twist operator. This is given most simply in terms of the response function

$$S_Q(\omega)=\sum_N|\langle N|Q|0\rangle|^2\delta(\omega-E_N)$$
$$=-\frac{1}{\pi}\text{Im}\langle 0|Q^+(\omega-H+i\eta)^{-1}Q|0\rangle \tag{18}$$

associated with a given one-body operator Q, which would be the twist operator in this specific case. As in Ref. 3 we attempt to calculate S_Q by matrix inversion in the full space of 1p-1h and 2p-2h states. This can be achieved by partitioning the matrix. Since Q will mainly connect the ground state to the 1p-1h states we only need the inverse matrix in the much smaller space of 1p-1h states alone

$$S_Q(\omega)=-\frac{1}{\pi}\text{Im}\langle 0|Q^+(1-P)(\omega-H_0-V+i\eta-VP(\omega-H_0-V+i\eta)^{-1}PV)^{-1}(1-P)Q|0\rangle\,. \tag{19}$$

P is a projector on the np-nh states with $n>1$.

Since the density of 2p-2h states in ^{208}Pb is around 1000/MeV we think it is quite safe to neglect the interaction V among these states. This, of course, is a considerable simplification because now $P(\omega-H_0+i\eta)^{-1}P$ is diagonal and may readily be inverted.

The microscpoic calculation therefore inverts the complex matrices

$$C_i=(1-P)(\omega_i-H_0-V+i\delta_1-VP(\omega_i-H_0+i\delta_2)PV)(1-P) \tag{20}$$

for a discrete set of energies $\{\omega_i\}$ with finite widths δ_1 and δ_2, and multiplies the inverse with the vectors Q and Q^+. In order not to miss any peaks located between the mesh points, ω_i, δ_1, and δ_2 must be finite and of the order of the mesh size. In principle we could choose $\delta_2>\delta_1$ compensating for the fact that we have neglected the interaction among the 2p-2h states. $\delta_2>\delta_1$ acknowledges our uncertainty about their actual position by distributing them over an energy range of order δ_2. In the calculation presented here, however, we will choose $\delta_2=\delta_1$ because the twist is actually far away from the 2p-2h states, so the exact position of the higher configurations will be of no importance. A diagrammatical decomposition of the interaction term coupling the higher configurations to the

one-particle-one-hole states distinguishes three classes of contributions: bubbles, ladders, and self-energy insertions. The first two link particle and hole lines together, whereas the self-energy insertions $M_i(\omega)$ are attached to a particle or a hole line alone. Therefore the latter also add to the unperturbed single particle energies e_i in the neighboring nuclei,

$$e_i = e_i^0 + \mathrm{Re}M_i(e_i) \ , \tag{21}$$

where, in principle, e_i now should correspond to the experimentally (or empirically) determined energies. Any realistic calculation needs single particle energies close to experiment in order to be successful. Practically, however, the fulfillment of (21) poses a formidable task unlikely to be accomplished. Condition (21) is enforced in this calculation by subtracting a constant term from the self-energy insertions

$$\mathrm{Re}M_i(\omega) \rightarrow \mathrm{Re}[M_i(\omega) - M_i(e_i)] + (e_i - e_i^0) \ . \tag{22}$$

Such or similar procedures clearly are essential for a correct description of states whose positions are dominated by single particle energies. The "unperturbed Hartree-Fock" energies e_i^0 appearing in (22) and representing H^0 in (19) and (20) are approximated by the empirical energies e_i divided by a state independent mass $m^*/m = 0.85$. This was found to be a fair approximation,[3] and limits the numerical efforts involved in the calculation.

What the manipulations on the single particle energies actually do is to make a guess on the unperturbed single particle energies. This guess is used in the propagators of the second order term. Together with the on shell part of the self-energy insertions, these unperturbed energies add up to the empirical ones.

The calculation performed uses a density dependent zero-range force for V in (20)

$$V = \{\rho V_{00}^{\mathrm{in}} + (1-\rho)V_{00}^{\mathrm{ex}} + \vec{\tau}_1 \cdot \vec{\tau}_2 [\rho V_{01}^{\mathrm{in}} + (1-\rho)V_{01}^{\mathrm{ex}}]\} \times \tfrac{1}{2}(1 - P_{12}^{\sigma} P_{12}^{\tau}) \delta(\vec{r}_{12}) \ . \tag{23}$$

The parameters are $V_{00}^{\mathrm{in}} = 53.6$, $V_{00}^{\mathrm{ex}} = -438.1$, $V_{01}^{\mathrm{in}} = 160.9$, and $V_{01}^{\mathrm{ex}} = 169.9$ (all in MeV fm^3), which are fairly close to the corresponding parameters in Landau-Migdal-type interactions (note, however, that the force is antisymmetrized here since higher configurations are explicitly taken into account). The interaction in (23) together with the single particle energies described earlier give the position and width of giant resonances in ^{90}Zr and ^{208}Pb up to a typical error of 1 MeV.[3]

IV. NUMERICAL RESULTS

Despite the large amount of numbers involved in the microscopic calculation, the most useful information resides in a single curve. So, Figs. 1–3 show our main result for the strength function in ^{208}Pb for three different operators. Figure 1 displays the response to

$$\hat{T}_{\mathrm{em}} = \sqrt{10/3\pi}\mu_{\mathrm{N}} \sum_i \tfrac{1}{2}(1+\tau_i^0)[\vec{r}_i \times \vec{1}_i]_2 \ , \tag{24}$$

Fig. 2 displays the response to $\hat{S}_{\mathrm{em}}$ given in the Introduction by (2). Figure 3 shows the total electromagnetic response to the $M2$ operator,

$$\hat{M}2 = \hat{T}_{\mathrm{em}} + \hat{S}_{\mathrm{em}} \ . \tag{25}$$

Each figure contains three curves and one smaller inset. The bottom graph in each shows the strength function for the case of no residual interaction at all, i.e., the Hamiltonian governing the motion is just made from single particle energies. The middle section displays the case where the residual interaction between 1p-1h configurations only is taken into account, whereas the upper curve gives the result of the full calculation coupling 2p-2h to the 1p-1h states. All three curves cover the energy range of 0–10 MeV. The inset in the top graph shows the result of the full calculation in the 1p-1h + 2p-2h space over the energy range 0–30 MeV; because of the larger mesh size there, a larger width has been chosen resulting in a smoothing of the strength functions. All curves are normalized to the total electromagnetic strength in the interval between 0 and 30 MeV which is $S = 3.7 \times 10^4 \ \mu_{\mathrm{N}}^2 \mathrm{fm}^2$ and almost exhausts the $M2$ sum rule.[2]

The most striking feature exhibited by our result is the sharp concentration of the twist strength around 7 MeV excitation energy (Fig. 1). This is very close to the 7.6 MeV predicted by the $45A^{-1/3}$ law derived in Sec. II. Furthermore, the concentration of twist strength is al-

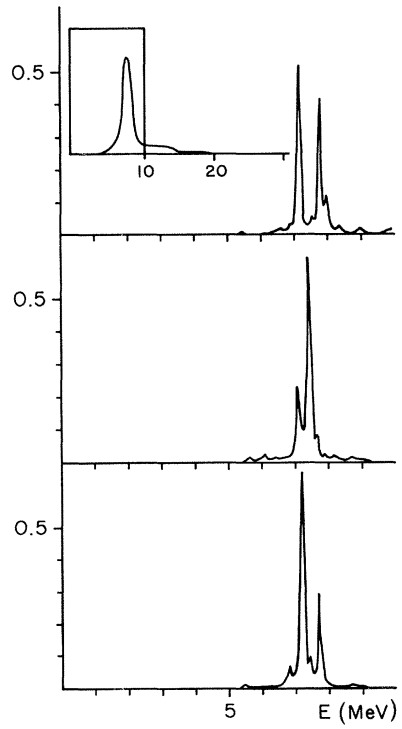

FIG. 1. Response of ^{208}Pb to the twist operator [Eq. (24)] in units of the total electromagnetic strength $S = 3.7 \times 10^4 \ \mu_{\mathrm{N}}^2 \mathrm{fm}^2$. The bottom part has no interaction; the middle part has interaction between 1p-1h only, and the top part has interaction between 1p-1h + 2p-2h; the inset shows the same response over a wider energy range.

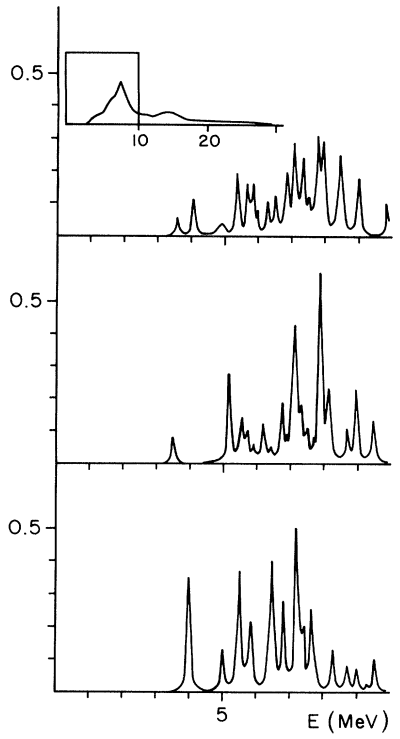

FIG. 2. Same as Fig. 1 for the spin flip operator [Eq. (2)].

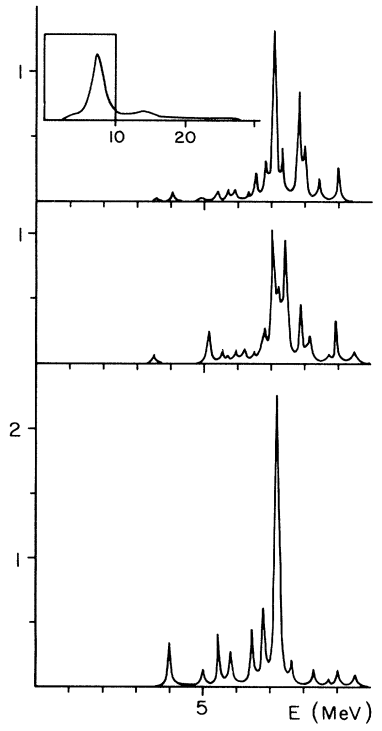

FIG. 3. Same as Fig. 1 for the electromagnetic $M2$ operator [Eq. (25)].

ready present in the single particle energies alone, with no residual interaction at all. Adding a residual interaction among the 1p-1h states has only little effect on the strength function and, actually, we have varied the strength and also individual components of the interaction over a large scale without moving the twist from its unperturbed position. Clearly this just reflects the findings from the fluid dynamical description that the energy of the twist does not depend on the Landau parameter F_0. Coupling the 2p-2h configurations to the 1p-1h states finally breaks the twist into two pieces, one at 7.2 MeV and one at 7.9 MeV. As far as the twist is concerned the microscopic calculation fully corroborates the fluid dynamical predictions.

Therefore let us examine the chances of detecting this mode, where we will now have to worry about the fact that the spin flip excitations will entirely[2] hide the resonance peaks coming from the twist, since they contribute 80% of the sum rule. Although the mean position of the spin flip modes is approximately at 7 MeV as predicted in (Ref. 2), their spread in energy is so large that the resonance peak from the twist is higher than any spin flip strength around 7 MeV.

The fragmentation of spin flip strength is already present with no residual interaction at all. The introduction of an interaction among the 1p-1h states tends to concentrate the spin flip modes around 7 MeV, but this tendency is actually reversed, once the coupling to 2p-2h configurations is added. The inset of Fig. 2 and Table I shows that 30% of the spin flip strength resides above 10 MeV. In fact, the amount of fragmentation of spin flip strength is most probably even underestimated because we have not included any mechanism usually used to explain fragmentation and quenching of magnetic strength, such as isobar-hole excitations.[10] Such mechanisms only affect the spin flip modes. Also, since we have used the bare g factors for the spin part of the $M2$ operator, we probably have overestimated the total $M2$ strength coming from this operator: Meson exchange effects are expected to quench these factors.[11] Finally, the effective G'_0 resulting from the antisymmetrized zero range interaction used here is too small. Any finite range interaction, which we had to discard because of computational limitations, would shift the spin flip states to higher energies. There they would suffer even more fragmentation since the density of 2p-2h states is higher there. All these mechanisms would of course enhance the relative importance of the twist to the $M2$ strength around 7 MeV.

The electromagnetic response calculated clearly reveals the contribution of the twist to the electromagnetic

TABLE I. Percentage of the sum rule strength from different operators and for different energy ranges. Experimental number is from Ref. 6.

Energy range	Twist	Spin flip	Electromagnetic	Experiment
[0,30]	18%	65%	92%	
[0,10]	14%	41%	65%	
[6,8]	10%	20%	39%	25%

strength function. The two prominent peaks at 7.2 and 7.9 MeV in the full calculation are just the two twist peaks sitting on a spin flip background. So, in contrast to the findings in Ref. 2, the twist mode in ^{208}Pb does not stand in the shadow of the spin flip. The reason for this is the enormous fragmentation of spin flip strength already present in the single particle energies.

Let us try to understand how this comes about numerically. There are 86 1p-1h states in our basis which can couple to $J^\pi=2^-$, 38 of them are proton *ph* states. Looking at the overlap of these *ph* states with the twist mode, we should not be surprised to find that *ph* states with high angular momentum give the biggest overlap:

(i) Since zl_z is a $1\hbar\omega$ operator it will only connect particles to holes in adjacent shells.

(ii) Since l_z does not change the angular momentum, only states with $\Delta l=1$ are connected by zl_z.

(iii) Since no spin flip is involved, $\Delta j=1$ is favored over $\Delta j=0,2$ for $\Delta l=1$.

(iv) A simple calculation actually yields

$$\langle 0\,|\,zl_z\,|\,([n,l+1],[n,l]^{-1})_{2^-,0}\rangle=\sum_m(-)^m\begin{bmatrix} l & l+1 & 2\\ m & -m & 0\end{bmatrix}\langle n,l,m\,|\,zl_z\,|\,n,l+1,m\rangle$$
$$=(-)^{l+1}\left[\frac{l(l+1)(l+2)(2l+3)}{15}\right]^{1/2} \tag{26}$$

for oscillator functions, showing that high angular momentum states are weighted by a factor $\sim l^2$.

Table II shows the most important particle hole states involved in the twist motion, their single particle energy, and their relative weight. Incidentally, the single particle energies for the most important configurations (denoted by an asterisk in Table II) are experimentally measured energies. Combining this with the fact that a residual interaction does not affect the position of the twist, this feature certainly contributes strongly to the significance of the results (single particle energies from the Skyrme interactions are rather different from these). Despite the fact that only a few *ph* configurations are important for the twist motion, they involve most of the 82 protons because of the high angular momenta involved.

In contrast to the twist motion, the spin flip operator does not weigh high angular momentum states because it is missing the operator l_z. Therefore the spin flip is dispersed over all 86 possible *ph* states, which also are spread over a much larger energy range.

These features also explain why our calculation in the case of ^{90}Zr does not show any concentration of twist strength, which is the reason why we do not present any figures for this nucleus. Primarily ^{90}Zr is not heavy enough to allow for the twist which, in the language just used, means that there are not enough states of sufficient high angular momentum available in ^{90}Zr. Furthermore, the single particle energies available are not given by experiment. This means that the uncertainties on the results for ^{90}Zr are much larger than in the case of ^{208}Pb. Finally the gap between particle and hole states is much smaller than in the case of lead, resulting in a heavier fragmentation of the strength function due to 2p-2h configurations. These three features make it very unlikely for ^{90}Zr to show a sharp resonance in response to a twisting field.

TABLE II. *ph* configurations participating in the twist motion.

p	*h*	*ph* energy	Relative weight
$*1i_{13/2}$	$*1h_{11/2}$	7.2	0.46
$*1h_{9/2}$	$1g_{7/2}$	7.7	0.31
$*2f_{7/2}$	$*2d_{5/2}$	6.8	0.11
$2f_{5/2}$	$*2d_{3/2}$	7.4	0.11

Let us finally mention the experimental findings on $M2$ strength from Refs. 5 and 6 which has been measured in the energy range of 6—8 MeV. The total strength there is reported to account for 25% of the sum rule. This is smaller than the 39% obtained here, but, as mentioned already, we have not introduced any mechanism to quench the $M2$ spin flip strength. These could easily account for the difference (the effective g factors used in the calculation accompanying the measurements in Ref. 5 reduce the spin flip strength by a factor of 0.58). Comparing individual peak positions calculated here with the measurements shows an embarrassing good agreement, which probably is accidental: The two largest peaks are found at 6.9 and 7.9 MeV, the one at 7.9 MeV being slightly smaller, displaying a double hump structure. Smaller peaks are seen at 6.5 and 7.5 MeV.

The calculation of Knüpfer *et al.* accompanying the measurements in Ref. 5 gives two major peaks around 7.5 and 9 MeV. Unfortunately, the results in Ref. 5 do not distinguish between orbital and spin flip excitations, making a comparison rather meaningless. We could guess that the 7.5 MeV state in Ref. 5 is predominantly twist, whereas the 9 MeV peak concentrates spin flip strength. The latter peak would be less pronounced in our case because of fragmentation due to the two-particle-two-hole coupling and because of less concentration due to a weak G'_0.

V. CONCLUSION

We have examined the question whether a microscopic description of nuclear excitations confirms semiclassical predictions on a collective twist motion. To this end we have derived specific properties of the excitation from the Landau theory and have shown that they also pertain on a

microscopic level. Our main result is that ^{208}Pb shows in response to the twist operator two very sharp resonances which are located at 7.2 and 7.9 MeV. The position of these states is entirely fixed by experimentally measured single particle energies because the residual interaction does not affect the position of transverse zero sound modes. According to our microscopic calculation the nucleus of ^{90}Zr is not heavy enough to exhibit a twisting motion.

We have also investigated the possibility of detecting the twist experimentally through electron scattering. Despite its overwhelming contribution to the $M2$ sum, the competing spin flip mode is so heavily fragmented that it cannot obscure the resonance peaks of the twist in an (e,e') scattering experiment. Therefore it seems safe to conclude that any major peak in the $M2$ response of ^{208}Pb around 7.5 MeV is mostly due to the twist.

The prominent peaks in the electromagnetic $M2$ strength calculated agree—most probably accidentally—perfectly with experimentally measured peaks in the energy range from 6 to 8 MeV. In order to confirm twist strength in experimentally observed peaks, a detailed study of the q dependence of these peaks would be necessary. We intend to investigate this point theoretically.

ACKNOWLEDGMENTS

I would like to thank J. Speth and the Kernforschungsanlage (KFA) Jülich, where part of this work was completed, for their hospitality and their support. This work was supported in part by US DOE Contract DE-AC 02-76 ER 13001 and by a fellowship from the Scientific Committee of NATO via the German Academic Exchange Service (DAAD).

[1]G. Holzwarth and G. Eckart, Z. Phys. A 283, 219 (1977).

[2]B. Schwesinger, K. Pingel, and G. Holzwarth, Nucl. Phys. A341, 1 (1980).

[3]B. Schwesinger and J. Wambach, Phys. Lett. 134B, 29 (1984); J. Wambach and B. Schwesinger, Proceedings of the International Symposium on Highly Excited States and Nuclear Structure, Orsay, 1983; B. Schwesinger and J. Wambach, Nucl. Phys. (to be published).

[4]T. Yukawa and G. Holzwarth, Nucl. Phys. A364, 29 (1981).

[5]R. Frey, A. Richter, A. Schwierczinski, E. Spamer, O. Titze, and W. Knüpfer, Phys. Lett. 74B, 45 (1978).

[6]W. Knüpfer, R. Frey, A. Friebel, W. Mettner, D. Meuer, A. Richter, E. Spamer, and O. Titze, Phys. Lett. 77B, 367 (1978).

[7]G. Baym and C. Pethick, *The Physics of Liquid and Solid Helium* (Wiley, New York, 1978), Part II, Ch. 1.

[8]A. R. Edmonds, *Angular Momentum in Quantum Mechanics*, 3rd ed., edited by R. Hofstadter (Princeton University, Princeton, N.J., 1974).

[9]G. Eckart, G. Holzwarth, and J. P. da Providencia, Nucl. Phys. A364, 1 (1981).

[10]M. Ericson A. Figureau, and C. Thévenet, Phys. Lett. 45B, 19 (1973); M. Rho. Nucl. Phys. A231, 493 (1974); K. Ohta and M. Wakamatsu, *ibid.* A234, 445 (1974).

[11]T. Yamazaki, in *Proceedings of the International Conference on Nuclear Structure and Spectroscopy, Amsterdam, the Netherlands, 1974,* edited by H. E. Blok and A. E. L. Dieperink (Scholars, Amsterdam, 1974), Vol. 1, p. 554.